Timing of abrupt climate change at the end of the Younger Dryas interval from thermally fractionated gases in polar ice

Jeffrey P. Severinghaus*, **Todd Sowers**†, **Edward J. Brook**‡, **Richard B. Alley**† & **Michael L. Bender***§

* *Graduate School of Oceanography, University of Rhode Island, Narragansett, Rhode Island 02882, USA*
† *Geosciences Department, Pennsylvania State University, University Park, Pennsylvania 16802, USA*
‡ *Departments of Geology and Environmental Science, Washington State University, Vancouver, Washington 98686, USA*

Rapid temperature change fractionates gas isotopes in unconsolidated snow, producing a signal that is preserved in trapped air bubbles as the snow forms ice. The fractionation of nitrogen and argon isotopes at the end of the Younger Dryas cold interval, recorded in Greenland ice, demonstrates that warming at this time was abrupt. This warming coincides with the onset of a prominent rise in atmospheric methane concentration, indicating that the climate change was synchronous (within a few decades) over a region of at least hemispheric extent, and providing constraints on previously proposed mechanisms of climate change at this time. The depth of the nitrogen-isotope signal relative to the depth of the climate change recorded in the ice matrix indicates that, during the Younger Dryas, the summit of Greenland was $15 \pm 3\,°C$ colder than today.

Abrupt changes in the Earth's climate system have generated much interest recently. Ice-core studies that infer palaeotemperature from the ratio of oxygen isotopes in the ice[1,2] and accumulation rate[3] have suggested that Greenland temperatures rose in less than a decade at the climate transition marking the end of the Younger Dryas cold interval and the beginning of the warmer Holocene epoch at 11.6 kyr before present, BP (here 'present' indicates AD 1950). Abrupt changes of similar age have appeared in other climate records over much of the globe. Whether these widespread changes were simultaneous, asynchronous, or unrelated has significant implications for our understanding of them, but dating uncertainties a century or more at present obscure these relationships.

One critical record of Younger Dryas climate change, also derived from ice cores, is the atmospheric methane concentration in trapped air. Analysis of the air trapped in bubbles in ice from Greenland[4–6] and from the Antarctic[7] has shown that atmospheric methane concentrations also increased near the end of the Younger Dryas. It is thought that this increase was in response to increased precipitation[4,5] and/or temperature[5] in the wetland methane source regions, which at that time were widely distributed over the tropics and possibly the middle- to high-latitude Northern Hemisphere[4,5,7]. Because the atmosphere is well mixed, its methane concentration serves as an integrator of methane sources (and thus climate information) over a broad spatial scale. As few methane sources existed in the North Atlantic basin during this period[5], a climate change that was restricted to this area alone could not have produced the observed atmospheric methane changes. Knowledge of the precise relative timing of the changes in temperature and methane should thus show whether the postulated abrupt Greenland temperature change was synchronous with climate change over a large portion of the Earth's terrestrial area. This information may in turn help constrain causal mechanisms of the abrupt changes.

Two problems currently prevent us from relating changes in temperature and methane in the ice core. First, the relationship between the $^{18}O/^{16}O$ ratio of ice ($\delta^{18}O_{ice}$) and the palaeotemperature

has been shown to vary with age[8,9], and we do not know the exact relationship at times of rapid climate change during the ice ages[10,11]. Recent borehole temperature studies[8] show that the $\delta^{18}O_{ice}$ 'palaeothermometer' underestimates the glacial-to-Holocene warming by about a factor of 2 when calibrated from the modern spatial $\delta^{18}O$–temperature relationship, motivating the search for an independent palaeothermometer. Second, the age of the air trapped in bubbles is less than the age of the enclosing ice because air is occluded at some depth below the surface of the ice sheet in the bubble close-off region[12–14]. This gas-age–ice-age difference is not known *a priori* for times past, making uncertain the relative timing of temperature and atmospheric gas changes[4,14].

Here we address these problems with a new technique for identifying rapid past temperature changes based on the principle of thermal diffusion, which fractionates gas mixtures in a temperature gradient according to their mass. The air in the porous unconsolidated layer of snow (firn) on top of polar ice sheets is fractioned by transient temperature gradients arising from abrupt climate change. This fractionated air is preserved in bubbles in glacial ice as a gas-isotope anomaly and thus serves as a gas-phase stratigraphic marker of the temperature–change event in an ice core. This approach circumvents the problem of the gas-age–ice-age difference by comparing gases directly with gases, enabling a precise determination of the relative time of local temperature changes and atmospheric gas changes. We apply the method to the GISP2 ice core from the summit of Greenland using the stable isotopes of N_2 and Ar in trapped air, and find that the increase in atmospheric methane concentrations at the end of the Younger Dryas interval began 0–30 years after an abrupt temperature increase. Where annual layers are countable[15], as in GISP2, the position of the gas-isotope anomaly relative to the record of the temperature event in the ice yields a precise estimate of the gas-age–ice-age difference, which allows a tie between atmospheric gas chronologies and the layer-counting timescale at times of abrupt change. We also use this age difference in conjunction with glaciological models[16,17] (which predict the depth and age of pore close-off in the firn) to obtain an estimate of absolute temperature that serves as a check

§ Present address: Department of Geosciences, Princeton University, New Jersey 08544, USA.

on the $\delta^{18}O_{ice}$ palaeothermometer. Finally, the relative changes in $^{15}N/^{14}N$ and $^{40}Ar/^{36}Ar$ confirm that the abrupt shift in $\delta^{18}O_{ice}$ at the Younger Dryas/Holocene transition was indeed a thermal event.

Thermal fractionation of air in the firn

A gas mixture subjected to a temperature gradient will tend to unmix by a process known as thermal diffusion[18,19]. The effect was predicted with the solution of the Boltzmann equation and the development of the kinetic theory of gases in 1911–17, which showed that diffusive molecular transport could be driven by a temperature gradient (thermal diffusion) in addition to a concentration gradient (concentration diffusion)[18]. Subsequently confirmed in the laboratory[20], the effect was studied extensively during the 1940s as a means to separate uranium isotopes. In a constant temperature gradient, a steady state is reached in which thermal diffusion in one direction is balanced by diffusion along a concentration gradient in the other direction. In this situation the difference in the isotope ratios R and R_o at temperatures T and T_o is given (in units of per mil) by theory as[19]

$$\delta = \left[R/R_o - 1\right]10^3 = \left(\left[T_o/T\right]^\alpha - 1\right)10^3 \qquad (1)$$

where δ is the fractional deviation of the isotope ratio R from the ratio R_o, T and T_o are temperature in K, and α is the thermal diffusion factor[18], a parameter characteristic of a pair of gas species. With a few exceptions, the heavier gas becomes enriched in the colder region[18]. For example, α for the isotopic pair $^{15}N^{14}N-^{14}N_2$ is about 0.0065 at 298 K (ref. 18), so a temperature gradient between 298 and 308 K will cause the cold end to have $\delta^{15}N = +0.2‰$ relative to the warm end. For comparison, our measurement precision for $\delta^{15}N$ in ice cores is $\pm0.02‰$ corresponding to $\pm1°C$. In our work, the gas at one end of the temperature gradient is always the free atmosphere at the top of the firn. The atmosphere is used as the reference for both $^{15}N/^{14}N$ and $^{40}Ar/^{36}Ar$ measurements, as these ratios are constant in air on the 10^4-year timescale relevant here[14,21].

A second process known as gravitational settling[22,23] also affects the gas composition in firn[14,24,25]. Separation of gases in an isothermal, porous column occurs according to the mass difference Δm alone as given by the barometric equation[24]

$$\delta = \left[R/R_o - 1\right]10^3 = \left(\exp\left[\Delta mgz/(R^*T)\right] - 1\right)10^3 \qquad (2)$$

where R is the isotopic ratio at depth z in the column, R_o is the ratio in air, g is the gravitational acceleration, R^* is the gas constant and δ is in units of per mil. For example, in a diffusive column of air 80 m thick at 236 K, the air at the bottom will have $\delta^{15}N = +0.4‰$ relative to the air at the top.

Observations of thermal diffusion in nature have thus far been limited to gas-filled porous media such as sand dunes[26] and firn[27], where advective mixing is inhibited by the small pore size such that transport is mainly by diffusion. These observations confirm that transient seasonal[26,27] and geothermal[26] temperature gradients fractionate air approximately as predicted.

After an abrupt climate warming, transient temperature gradients lasting several hundred years should arise in the upper part of the firn owing to the thermal inertia of the underlying firn and ice. The heavy gas species such as $^{15}N^{14}N$ and ^{40}Ar should therefore be preferentially driven downwards, towards the cold deeper firn, relative to the lighter species ($^{14}N_2$ and ^{36}Ar). An important point is that gases diffuse about 10 times faster than heat in firn[28], so the thermally fractionated gas will penetrate to the bottom of the firn long before the temperature equilibrates, and the gas composition will closely approach a steady state with respect to the firn temperature such that equation (1) should be valid. Figure 1 shows model results of the expected firn-air composition in the 50 years following a 5°C 'step function' increase in surface temperature (see Methods). We note that the isotopic signal propagates to the bottom

of the firn during the first decade, superimposed on the linear downward increase in $\delta^{15}N$ due to gravitational settling. By 50 years after the initial warming, $\delta^{15}N$ at the bottom of the firn rises to the steady-state value of thermal fractionation (the signal is not attenuated at this time). As the bubbles close off they trap a sample of the basal firn air, thus recording the thermal event as a heavy-gas anomaly in the bubble air composition. Changes in atmospheric methane concentrations should also propagate downwards at the same speed, with a slight correction for the fact that CH_4 diffuses ~7% faster than $^{15}N^{14}N$. These CH_4 variations will be trapped in the bubbles along with the thermal signal, allowing a precise estimate to be obtained of the temporal relationship between the abrupt change
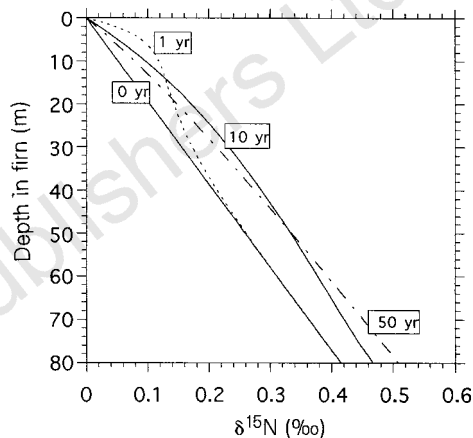
Figure 1 Results of a heat and molecular diffusion model of gas in polar firn. This model was used to simulate the effect on firn-air isotopic composition of a 5°C 'step function' increase in surface temperature (constant temperature before and after the step). $\delta^{15}N \equiv [(^{15}N/^{14}N_{sample})/(^{15}N/^{14}N_{atmosphere}) - 1]10^3$, where $\delta^{15}N$ is in units of per mil. The time in years after the step is shown by the numbers in boxes. See Methods section for model architecture.
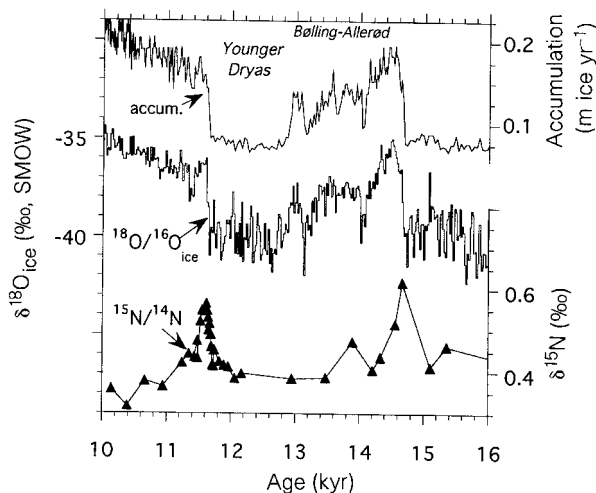

Figure 2 GISP2 records of accumulation[9], $\delta^{18}O_{ice}$ (ref. 2), and $\delta^{15}N$ of trapped air (ref. 47 and this work) covering the last deglaciation. Age values for $\delta^{15}N$ were obtained from a model estimate[17] of the gas-age–ice-age difference and may be in error by ~100 yr. Means of replicate $\delta^{15}N$ measurements are shown. Note the $\delta^{15}N$ anomaly of about +0.15‰ at 11.6 kyr BP, followed by a decline after several hundred years. An even larger anomaly appears to be present at the beginning of the Bølling-Allerød and is the subject of current work. The abrupt cooling at the beginning of the Younger Dryas is expected to produce a negative anomaly in $\delta^{15}N$, the apparent absence of which may reflect low sampling resolution in that interval.

in surface temperature and the CH_4 increase. Further modelling shows that after several hundred years the thermal diffusion anomaly decays as the firn becomes isothermal. In the case of a warming, the $\delta^{15}N$ anomaly observed in ice cores should thus take the form of a sudden increase followed by a gradual decrease. Sudden cooling is expected to produce the opposite effect.

Observations of nitrogen and methane in trapped air

As can be seen Fig. 2, $\delta^{15}N$ in the GISP2 ice core during periods of cold, stable climate is about +0.4‰, the expected value for gravitational settling with a firn thickness of ~80 m. The end of the Younger Dryas interval at 11.6 kyr BP is identified by the abrupt

increase in $\delta^{18}O_{ice}$. At this point the $\delta^{15}N$ record shows a 'spike' to +0.56‰, followed by a decay over several hundred years. A similar anomaly is seen in the $^{18}O/^{16}O$ ratio of O_2 (not shown), with twice the amplitude of the $\delta^{15}N$ anomaly, as expected from reported values of the thermal diffusion factor[18]. Figure 3a shows an expanded view of the $\delta^{15}N$ anomaly plotted versus depth in the ice. We interpret the sudden rise in $\delta^{15}N$ at ~1,700 m depth as the gas-phase marker of the climate event. By minimizing the mis-match between model $\delta^{15}N$ (Fig. 4) and the data, we assign the event age[3] of 11.64 kyr BP to the gas at 1,700.3 m, with an estimated depth uncertainty corresponding to ±20 yr (based on the sample resolution).
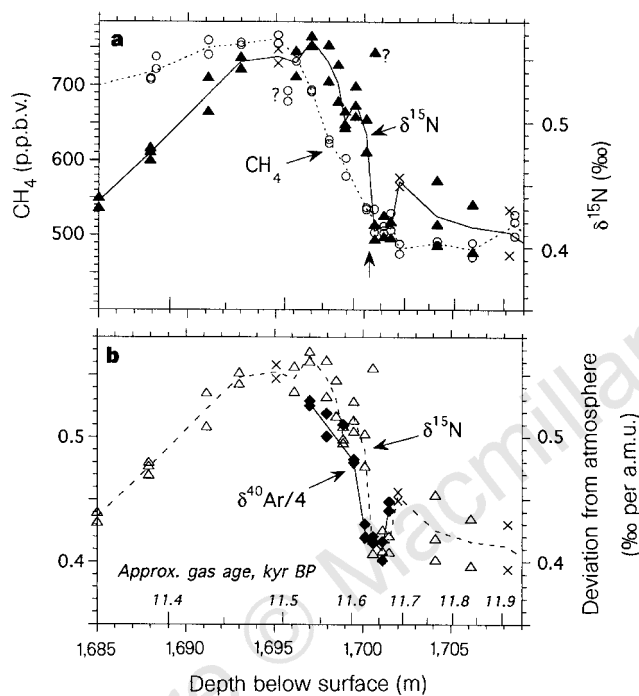
Figure 3 Gas data from GISP2 covering the end of the Younger Dryas, plotted versus depth. **a**, Expanded view of the $\delta^{15}N$ anomaly in Fig. 2 showing individual replicates, with methane data superimposed for comparison. Lines pass through the means of replicates, except for a pair of methane points at 1,695.7 m which we consider to be anomalous. We reject the $\delta^{15}N$ outlier at 1,700.6 m and draw the line through the mean of the remaining two replicates. Cross symbols (×) denote $\delta^{15}N$ measurements made in an earlier study[47]. Note the sharp increase in $\delta^{15}N$ at ~1,700 m depth from the baseline value of +0.4‰ to +0.5‰. Samples spanning this change are 18 yr apart, placing an upper limit on the amount of smoothing and hence the duration of the air enclosure process. We interpret the inflection point in $\delta^{15}N$ at 1,700.3 m (arrow) as a marker of the thermal event in the gas phase. The $\delta^{15}N$ outlier at 1,700.6 m makes the location of the inflection point ambiguous, so we accept a location error corresponding to one sample spacing. For reference, approximate gas age is plotted along the horizontal axis, adjusted to be consistent with our conclusion that the $\delta^{15}N$ anomaly began at 11.64 kyr BP. **b**, $\delta^{40}Ar/4$ in ice adjacent to the $\delta^{15}N$ samples, superimposed on the $\delta^{15}N$ data for comparison. $\delta^{40}Ar \equiv [(^{40}Ar/^{36}Ar_{sample})/(^{40}Ar/^{36}Ar_{atmosphere}) - 1]10^3$, where $\delta^{40}Ar$ is in units of per mil. $\delta^{40}Ar$ is divided by four for comparison with $\delta^{15}N$ due to the four mass unit difference between ^{40}Ar and ^{36}Ar; gravitational fractionation is the same for all isotopes on a per mass unit basis. Lines connect means of replicate points. Note the rough agreement of Ar and N_2 at depths >1,700 m, implying that gravitation is the only process at work. In contrast, at depths <1,700 m $\delta^{40}Ar/4$ data fall below $\delta^{15}N$ data, with the exception of the single (unreplicated) Ar point at 1,698.8 m. Integrity of this sample may have been compromised because it came from the outer 2 cm of the core. The lower $\delta^{40}Ar/4$ requires a thermal fractionation component in the points at 1,697, 1,698, 1,699.5 and 1,700 m. Note unexplained discrepancies of ~0.03‰ in samples from 1,700 and 1,701.5 depth (a.m.u., atomic mass unit).
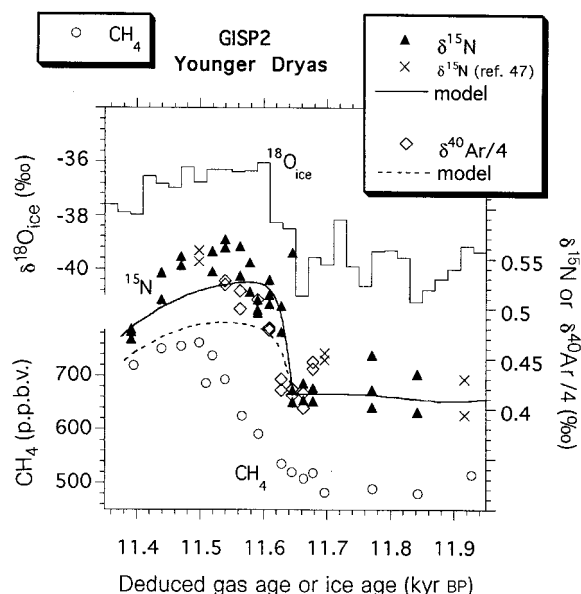
Figure 4 Isotopic and CH_4 data plotted versus age derived by this work. Bidecadal mean $\delta^{18}O_{ice}$ (ref. 2) is shown for comparison (top). Model $\delta^{15}N$ (solid line) is the result of a simulation forced by a 5 °C linear increase in surface temperature over the 10-yr period from 11.64 to 11.63 kyr BP, with constant temperature before and after these times. Only the relative changes in the model have significance; model absolute values are arbitrary and are forced to go through the mean (+0.415‰) of the six observed $\delta^{15}N$ values at 11.64–11.68 kyr BP (the outlier at 11.64 kyr BP is excluded). The gravitational effect of column deepening is added to the model curve using model[17] predicted firn thickness changes (this effect reaches a maximum of +0.034‰ per mass unit at 11.5 kyr BP). The age scale was derived by assuming that the gas age at 1,700.3 m is 11.64 kyr BP, and calculating ages relative to this point from gas-age–ice-age differences predicted by a dynamic densification model[17].

Methane concentration analyses[5] of air trapped in bubbles are superimposed for comparison in Fig. 3a. Methane concentration first rises significantly beyond the envelope of Younger Dryas variability (± 30 parts per billion by volume, p.p.b.v.) at 1,699 m depth, which is ~30 years after the corresponding increase in $\delta^{15}N$ at 1,700.1 m depth. Because there are no CH_4 samples between these depths, we infer that atmospheric methane began to rise 0–30 years after the warming event. Allowance for the slightly faster diffusion of CH_4 than $^{15}N/^{14}N$ makes the zero-year lag slightly less likely. Importantly, methane rises more gradually than $\delta^{15}N$, taking >150 years to reach maximum values. In contrast, modelling of the rapid $\delta^{15}N$ change between 1.700.6 and 1,700.1 m suggests a step-like temperature change that occurred in less than a decade (Fig. 4).

Separation of thermal and gravity effects

It is likely that the $\delta^{15}N$ anomaly at 11.6–11.4 kyr BP is partly due to a sudden deepening of the diffusive firn column and the resulting increase in gravitational settling. A transient deepening of the firn is expected owing to the doubled accumulation rate[3] at this time. A dynamic densification model[17] predicts 6 m of deepening, which would increase $\delta^{15}N$ by 0.03‰. Wind speed also may have dropped at this time[29,30], which could have decreased the thickness of a near-surface convective zone[31] in which gravitational separation is prevented by wind-pumping[32], thereby deepening the diffusive column. To address the issue of how much of the isotopic signal is due to temperature change, we exploit the fact that Ar is half as sensitive to thermal fractionation as N_2 (ref. 18). This allows us to separate thermal and gravitational effects by measurement of N_2 and Ar isotopes in the same ice. If the $\delta^{15}N$ anomaly is due entirely to increased gravitational settling, then Ar isotopes should show an anomaly with the same amplitude as N_2 isotopes, when scaled by mass difference (that is, $\delta^{40}Ar/4$ should equal $\delta^{15}N$). On the other hand, if the anomaly is due entirely to thermal fractionation then $\delta^{40}Ar/4$ should change only half as much as $\delta^{15}N$.

Figure 3b shows $\delta^{40}Ar/4$ from ice samples at the same depths as the $\delta^{15}N$ samples. The anomaly in Ar appears to be less than that of N_2, and therefore we conclude that the anomaly marks a thermal fractionation event. Because the Ar amplitude is about 3/4 rather than 1/2 of the N_2 amplitude, the anomaly must also be partly due to gravitation via diffusive column deepening. A preliminary quantification of the thermal and gravity components gives 5–10 °C of abrupt warming, possibly followed by a gradual column deepening over a century. We consider these estimates highly tentative.

Analytical uncertainties are large, and the thermal diffusion factors for N_2 and Ar at −40 °C remain to be measured. The possibility remains that part of the abrupt $\delta^{18}O_{ice}$ increase at 11.6 kyr BP was due to a geographical shift[11,33–35] in the location of the moisture source rather than a warming at the drill site (summit).

Climatic implications of methane trends

Using the $\delta^{15}N$ anomaly as a stratigraphic marker of the warming event, we conclude that the methane increase began 0–30 years after the warming at Summit. Subsequently, however, methane increased more slowly than the temperature such that the bulk of the methane increase came after the warming (Fig. 4). Therefore a causal role for methane in the warming, already doubtful owing to the small greenhouse effect of methane[6], is clearly ruled out by these phase data. Instead, methane seems to be responding to the climate change. The dominant source of atmospheric methane in the pre-industrial period was wetlands[36]. Because changes in sink strength are thought to have been small[37], atmospheric concentration variations are thought to primarily reflect variations in wetland temperature[5] and/or wetland area and hence terrestrial precipitation minus evaporation[4,36]. Because the residence time of methane in the atmosphere is about a decade[38], changes in the methane source could have preceded the observed atmospheric change by no more than a decade. As noted previously (but with less resolution)[4,5], the near synchroneity of the methane and temperature changes and the widespread distribution of methane sources imply that this climate event was at least hemispheric in extent. Furthermore, the speed of the apparent link between methane source regions and Greenland is evidence supporting an atmospheric transmission of the climate signal, as transmission through the ocean would have been too slow.

Our results may have implications for a proposed link[39] between changes in the tropical hydrological cycle and North Atlantic deep water (NADW) formation. An increase in the net evaporation rate over the tropical Atlantic might increase the salinity of poleward-bound subtropical surface water and hence increase NADW formation[39], as well as increasing precipitation over land[4]. An increase in NADW formation is widely thought to have caused the abrupt Greenland warming[40]. If an increase in tropical precipitation induced the atmospheric methane rise, methane might be expected to lead the Greenland warming by the amount of time required for saline water to make its way from the tropics to the North Atlantic[4] (several decades). Our results do not provide

---

Table 1 Palaeothermometry based on observed gas-age–ice-age difference

| | Input parameters | | | Greenland summit temperature (°C) | | | |
| | | Density | | | | $\delta^{18}O$ thermometer | |
	Δage (yr)	Accumulation (m H₂O yr⁻¹)	Lock-in (kg m⁻³)	Initial (kg m⁻³)	This work	Measured	Borehole-based (ref. 8)	Spatial gradient-based
Present (GLSP2 site, ref. 17)	195	0.227	814	350	−30	−31		
Younger Dryas (GISP2 site)	809*	0.073†	820‡	360§	−46‖		−47	−39
1σ error	±20	±0.01	±15	±10	±3			
Sensitivity test for lock-in density	809	0.073	810	360	−47.3			
	809	0.073	835	360	−43.7			

The last two columns at the right show, for comparison, the temperatures estimated using the traditional oxygen isotope palaeothermometer for two different calibrations ($d\delta/dT$) based on borehole thermometry (0.33) and the modern spatial covariation of $\delta^{18}O$ with temperature (0.65). The latter neglects changes in seawater $\delta^{18}O$ due to ice volume change. The input parameters chosen imply that Younger Dryas lock-in depth was 92 m (ref. 16). For comparison, the height of the firn diffusive column inferred from the Younger Dryas mean $\delta^{15}N$ of +0.415‰ (Fig. 3) and equation (2) is 80 m. The discrepancy could be due to the presence of a ~12-m-thick near-surface zone that was well flushed by wind-pumping (refs 31, 32).
* This work.
† Ref. 9. This is the mean value for the last 400 years of the Younger Dryas, for the scenario of 200 km of net ice margin retreat during deglaciation. Error is subjective and is based on model scenarios (K. Cuffey, personal communication).
‡ Calculated from ref. 17; also equal to South Pole present value (ref. 42). Error is subjective and is based on the range of published estimates.
§ Value used in Fig. 2 in ref. 16. Error is subjective. The result is nearly insensitive to this parameter.
‖ Error includes contribution from scatter in the Herron-Langway model (Fig. 1 in ref. 16). The model predicts modern temperature with 1σ error of ±2 °C (see text). To include this error in our result, we assign an error to the prefactor (575) of the rate constant k_1 in ref. 16. We then adjust this error until it produces a ±2 °C error in the result, with all other errors set to zero. The resulting prefactor error is ±60, which is then propagated in the Monte Carlo method along with the other four errors.

support for such a link inasmuch as methane does not appear to lead temperature at this one warming event.

Palaeothermometry from stratigraphic marker position

We can also use the $\delta^{15}N$ anomaly at the beginning of the Younger Dryas termination as a palaeothermometer. Colder temperatures slow the sintering of firn into ice because it is a temperature-activated metamorphic process[16]. The age of the ice at which air is trapped depends on firn temperature and ice accumulation rate[16]. In GISP2 there are 809 ± 20 annual layers[3,15] between the beginning of the $\delta^{15}N$ increase (1,700.3 m depth) and the shift in $\delta^{18}O_{ice}$ that marks the warming in the solid phase. An age difference of 809 years and an accumulation rate of 0.073 m water yr^{-1} (refs 3, 9) imply a temperature of $-46 \pm 3\,^\circ C$ (Table 1), which is $15 \pm 3\,^\circ C$ colder than at present (this calculation assumes steady-state before the termination). To check the method we use it to estimate modern temperature at Summit; we obtain $-30\,^\circ C$ which is close to the measured value of $-31\,^\circ C$.

This estimated temperature of $-46 \pm 3\,^\circ C$ agrees well with the borehole temperature-based estimate of $-47\,^\circ C$ for this time[8], but is significantly colder than the value inferred from the spatially calibrated $\delta^{18}O_{ice}$ palaeothermometer (ref. 35; Table 1). (We point out that mean tropospheric temperature might not have been $15\,^\circ C$ colder than at present if the near-surface atmospheric inversion layers common on polar ice sheets were stronger at Summit during the Younger Dryas interval[9].)

This $15\,^\circ C$ temperature change is not inconsistent with the figure of $5-10\,^\circ C$ noted earlier for the amount of abrupt warming, because of the very different time spans involved. The entire transition from Younger Dryas to typical Holocene $\delta^{18}O_{ice}$ values took $\sim 1,500$ years (Fig. 2), over which time the $15\,^\circ C$ change probably occurred, whereas the $5-10\,^\circ C$ figure applies to a 'step' change that occurred over several decades or less. In this context we note that the thermal diffusion tool is not sensitive to gradual temperature change ($< 0.01\,^\circ C\,yr^{-1}$), because the firn becomes isothermal on a timescale of several hundred years. □

Methods

Analytical. Samples of ice were analysed respectively for N_2 (10-g samples) and Ar (35-g samples) isotopic composition with a melt-refreeze technique that releases the air trapped in bubbles[14]. Ice was generally taken from the central portion of the core to minimize possible adverse effects of gas loss due to temperature fluctuations during core retrieval and handling. N_2 isotopes were measured as in ref. 14. Air for Ar analysis was extracted in two melt-refreeze cycles to increase yield, and the air was exposed to a Zr/Al SAES getter at 900 $^\circ C$ for 10 min removing all the N_2, O_2 and other reactive gases. Pure N_2 equal to 10× the residual Ar was then added to increase sample volume to improve mass spectrometry, and the ratio of mass 40 to mass 36 of the mixture was measured on a multi-collector Finnigan MAT 252 mass spectrometer. Corrections of the order of 0.01‰ were made for the sensitivity of the relative ionization efficiencies of ^{40}Ar and ^{36}Ar in the mass spectrometer source to variations in the Ar/N_2 ratio and to pressure imbalance between sample and reference inlets. The standard deviation from the mean of replicate ice samples cut from the same depth was $\pm 0.02‰$ for $\delta^{15}N$, and $\pm 0.03‰$ for $\delta^{40}Ar$ (or $\pm 0.008‰$ on a per mass unit difference basis). Analytical precision for analyses of firn air is about $\pm 0.01‰$ for both $\delta^{15}N$ and $\delta^{40}Ar$, suggesting that the larger variability in the ice-core results was due either to artefacts introduced during the sample extraction procedure or real sample-scale heterogeneities in the ice. Simulated extractions were performed by introducing a sample of dry Rhode Island air to the extraction vessel over thoroughly degassed GISP2 ice, then following the normal extraction procedure. Results of these experiments revealed no systematic bias resulting from the extraction procedure. Methane procedures and results are described elsewhere[5].

Numerical simulation. A time-dependent gas diffusion model forced by an independent heat advection–diffusion model was used to explore the magnitude and shape of the expected firn-air and ice-core isotopic anomaly resulting from sudden climate change. Advection of molecules was neglected.

Three processes were treated in the gas diffusion model: concentration diffusion (Fick's Law), thermal diffusion, and gravitational settling. Gas fluxes were calculated from the difference between the concentration gradient and the thermal/gravitational equilibrium gradient, in effect relaxing the concentrations back to the equilibrium profile at the rate given by the diffusivity (following ref. 26). Justification for this approach is based on the fact that thermal diffusion proceeds at the speed of concentration diffusion[20] and is further discussed in ref. 41. Model gas diffusivities decreased monotonically downward in the firn, and were prescribed based on an assumed density profile and an empirical density–diffusivity relation derived from CO_2 measurements in South Pole firn air[42]. The firn–ice transition was held constant at 80 m and treated as an impermeable boundary condition. The heat model was adapted from ref. 43. Thermal conductivity and heat capacity were scaled to density based on empirical data. The insulating bottom boundary of the heat model was extended to 800 m depth to account for the thermal inertia of the ice. The initial condition of the model was isothermal at 227 K, and the model was forced at the upper boundary condition with a 5 $^\circ C$ step function.

Palaeotemperature inversion. Herron and Langway[16] showed that firn densification is a function of temperature and snow accumulation rate, and constructed an empirical model of the densification process based on measured density–depth profiles from 17 locations in Greenland and Antarctica with firn temperatures at 10 m depth ranging from -15 to $-57\,^\circ C$ and accumulation rates ranging from 0.5 to 0.02 m water yr^{-1}. Using their regression coefficients, we are able to predict modern temperature (T) at these 17 sites from the given accumulation (A) and density–depth ($d\rho/dz$) data to within $\pm 2\,^\circ C$ (1σ) of the measured temperatures, suggesting the potential usefulness of the model as a palaeothermometer.

The layer-counting age of our inferred gas-phase temperature change marker at 1,700.3 m is 12,449 yr (ref. 15), compared to the layer-counting age of 11,640 yr of the climate event as recorded in the ice by $\delta^{18}O_{ice}$ (ref. 2), electrical conductivity[44] and accumulation[3], giving an inferred gas-age–ice-age difference (Δage) of 809 yr. We adopt a subjective uncertainty of ± 20 yr based on the $\delta^{15}N$ sample spacing of ~ 18 yr (Fig. 3a) and the ambiguity introduced into our interpretation of the depth of the $\delta^{15}N$ inflection point by a single outlier at 1,700.58 m (Fig. 3a). Relative uncertainty in the layer counting in this interval is of the order of 1% or ~ 8 yr (ref. 15).

To relate this value of Δage to the Herron–Langway model, we assume that gases are cut off from mixing with the atmosphere at a specified density known as the lock-in density[13,42] (ρ_L). This assumption is predicated on observations of firn air that show that at most sites air is cut off from mixing with the atmosphere by impermeable high-density winter layers before the bubbles are all closed[13,25,42,45,46]. We also must specify an initial density at the surface (ρ_o), which has little effect on the result. Accumulation is from Cuffey and Clow's[9] corrections for thinning to measurements of layer thickness using a coupled ice and heat flow model. We solve equations (11) and (9) in Herron and Langway[16] to obtain T (in K) as an iteratively solved function of Δage, A, ρ_L and ρ_o:

$$T = \frac{21400}{R^*} \Bigg/ \ln\left\{ \frac{575A^{0.5}}{\ln\left[\frac{\rho_i - 550}{\rho_i - \rho_L}\right]} \left([\Delta\text{age} + \tau_{air}] - \frac{\exp\left[\frac{10160}{R^*T}\right]\ln\left[\frac{\rho_i - \rho_o}{\rho_i - 550}\right]}{11A} \right) \right\}$$

(3)

where R^* is the universal gas constant (8.314 J mol^{-1} K^{-1}), ρ_i is the density of ice (917 kg m^{-3}) and τ_{air} is the age of air in firn at lock-in, 15 yr (calculated based on ref. 17).

An important assumption for this approach to be valid is that the densification process was at steady state. We take the constancy of $^{18}O_{ice}$ and accumulation[9] during the Younger Dryas period as an indication that this assumption is warranted. Uncertainties are propagated assuming that they are uncorrelated and normally distributed via a Monte Carlo method. The largest source of uncertainty in the result arises from poor knowledge of the lock-in density ρ_L. Schwander[25] estimated this value at 795–800 kg m^{-3}, although at very low accumulation rates it may increase due to breakup of annual layers by wind erosion[25]. We adopt a value of 820 kg m^{-3} based on an empirical formula[17,45] for the variation of ρ_L with temperature, and note that the present value at the South Pole inferred from firn air $\delta^{15}N$ is 820 ± 5 kg m^{-3} (ref. 42; M. Battle, personal communication) and conditions (A and T) there are similar to

those inferred for the GISP2 site during Younger Dryas time[8]. We note that Greenland summit was not among the 17 sites used to develop the Herron–Langway model, so there is no circularity in our use of the GISP2 site as test of the method's ability to predict modern temperature.

1. Johnsen, S. J. et al. Irregular glacial interstadials recorded in a new Greenland ice core. Nature 359, 311–313 (1992).
2. Stuiver, M., Groetes, P. M. & Braziunas, T. F. The GISP2 δ^{18}O climate record of the past 16,500 years and the role of the sun, ocean, and volcanoes. Quat. Res. 44, 341–354 (1995).
3. Alley, R. B. et al. Abrupt increase in Greenland snow accumulation at the end of the Younger Dryas event. Nature 362, 527–529 (1993).
4. Chappellaz, J. et al. Synchronous changes in atmospheric CH_4 and Greenland climate between 40 and 8 kyr BP. Nature 366, 443–445 (1993).
5. Brook, E. J., Sowers, T. & Orchardo, J. Rapid variations in atmospheric methane concentration during the past 110,000 years. Science 273, 1087–1093 (1996).
6. Chappellaz, J., Barnela, J.-M., Raymond, D., Korotkevich, Y. S. & Lorius, C. Ice-core record of atmospheric methane over the past 160,000 years. Nature 345, 127–131 (1990).
7. Chappellaz, J. et al. Changes in the atmospheric CH_4 gradient between Greenland and Antarctica during the Holocene. J. Geophys. Res. 102, 15987–15997 (1997).
8. Cuffey, K. M. et al. Large Arctic temperature change at the Wisconsin-Holocene glacial transition. Science 270, 455–458 (1995).
9. Cuffey, K. M. & Clow, G. D. Temperature, accumulation, and ice sheet elevation in central Greenland through the last deglacial transition. J. Geophys. Res. 102, 26383–26396 (1997).
10. Jouzel, J. et al. Validity of the temperature reconstruction from water isotopes in ice cores. J. Geophys. Res. 102, 26471–26487 (1997).
11. Charles, C., Rind, D., Jouzel, J., Koster, R. D. & Fairbanks, R. G. Glacial-interglacial changes in moisture sources for Greenland: Influences on the ice core record of climate. Science 263, 508–511 (1994).
12. Schwander, J., Stauffer, B. & Sigg, A. Air mixing in firn and the age of the air at pore close-off. Ann. Glaciol. 10, 141–145 (1988).
13. Schwander, J. et al. The age of the air in the firn and the ice at summit, Greenland. J. Geophys. Res. 98, 2831–2838 (1993).
14. Sowers, T., Bender, M. & Raynaud, D. Elemental and isotopic composition of occluded O_2 and N_2 in polar ice. J. Geophys. Res. 94, 5137–5150 (1989).
15. Meese, D. A. et al. The Greenland Ice Sheet Project 2 depth-age scale: Methods and results. J. Geophys. Res. 102, 26411–26423 (1997).
16. Herron, M. M. & Langway, C. C. Firn densification: An empirical model. J. Glaciol. 25, 373–385 (1980).
17. Schwander, J. et al. Age scale of the air in the summit ice: Implication for glacial-interglacial temperature change. J. Geophys. Res. 102, 19483–19494 (1997).
18. Grew, K. E. & Ibbs, T. L. Thermal Diffusion in Gases (Cambridge Univ. Press, 1952).
19. Chapman, S. & Cowling, T. G. The Mathematical Theory of Non-Uniform Gases (Cambridge Univ. Press, 1970).
20. Chapman, S. & Dootson, F. W. A note on thermal diffusion. Phil. Mag. 33, 248–253 (1917).
21. Mariotti, A. Atmospheric nitrogen is a reliable standard for natural ^{15}N abundance measurements. Nature 303, 685–687 (1983).
22. Dalton, J. On the constitution of the atmosphere. Phil. Trans. Part 1, 174–187 (1826).
23. Gibbs, J. W. Collected Works Vol. 1, Thermodynamics (Yale Univ. Press, New Haven, 1928).
24. Craig, H., Horibe, Y. & Sowers, T. Gravitational separation of gases and isotopes in polar ice caps. Science 242, 1675–1678 (1988).
25. Schwander, J. in The Environmental Record in Glaciers and Ice Sheets (eds Oeschger, H. & Langway, C.) 53–67 (Wiley, New York, 1989).
26. Severinghaus, J. P., Bender, M. L., Keeling, R. F. & Broecker, W. S. Fractionation of soil gases by diffusion of water vapor, gravitational settling, and thermal diffusion. Geochim. Cosmochim. Acta 60, 1005–1018 (1996).
27. Severinghaus, J. P. & Sowers, T. Thermal diffusion as a temperature-change indicator in ice core climate records. (abstr.) Eos 76, F291 (1995).
28. Paterson, W. S. B. The Physics of Glaciers (Pergamon, Oxford, 1969).
29. Mayewski, P. A. et al. The atmosphere during the Younger Dryas. Science 261, 195–197 (1993).
30. Alley, R. B. et al. Changes in continental and sea-salt atmospheric loadings in central Greenland through the most recent deglaciation. J. Glaciol. 41, 503–514 (1995).
31. Sowers, T., Bender, M., Raynaud, D. & Korotkevich, Y. S. δ^{15}N of N_2 in air trapped in polar ice: A tracer of gas transport in the firn and a possible constraint on ice age-gas age differences. J. Geophys. Res. 97, 15683–15697 (1992).
32. Colbeck, S. C. Air movement in snow due to windpumping. J. Glaciol. 35, 209–213 (1989).
33. Johnsen, S. J., Dansgaard, W. & White, J. W. C. The origin of Arctic precipitation under present and glacial conditions. Tellus B 41, 452–468 (1989).
34. Fairbanks, R. G. The age and origin of the "Younger Dryas climate event" in Greenland ice cores. Paleoceanography 5, 937–948 (1990).
35. Dansgaard, W., White, J. W. C. & Johnsen, S. J. The abrupt termination of the Younger Dryas climate event. Nature 339, 532–534 (1989).
36. Chappellaz, J., Fung, J. Y. & Thompson, A. M. The atmospheric CH_4 increase since the Last Glacial Maximum. Tellus B 45, 242–257 (1993).
37. Martinerie, P., Brasseur, G. P. & Granier, C. The chemical composition of ancient atmospheres: A model study constrained by ice core data. J. Geophys. Res. 100, 14291–14304 (1995).
38. Prinn, R. G. et al. Atmospheric trends and lifetime of CH_3CCl_3 and global OH concentrations. Science 269, 187–192 (1995).
39. Duplessy, J. C. et al. Changes in surface salinity of the North Atlantic Ocean during the last deglaciation. Nature 358, 485–488 (1992).
40. Broecker, W. S. & Denton, G. H. The role of ocean-atmosphere reorganizations in glacial cycles. Geochim. Cosmochim. Acta. 53, 2465–2501 (1989).
41. Bender, M. L., Sewers, T., Barnola, J.-M. & Chappellaz, J. Changes in the O_2/N_2 ratio of the atmosphere during recent decades reflected in the composition of air in the firn at Vostok Station, Antarctica. Geophys. Res. Lett. 21, 189–192 (1994).
42. Battle, M. et al. Atmospheric gas concentrations over the past century measured in air from firn at the South Pole. Nature 383, 231–235 (1996).
43. Alley, R. B. & Koci, B. R. Recent warming in central Greenland? Ann. Glaciol. 14, 6–8 (1990).
44. Taylor, K. C. et al. The 'flickering switch' of late Pleistocene climate change. Nature 361, 432–436 (1993).
45. Martinerie, P., Raynaud, D., Etheridge, D. M., Barnola, J.-M. & Mazaudier, D. Physical and climatic parameters which influence the air content in polar ice. Earth Planet. Sci. Lett. 112, 1–13 (1992).
46. Etheridge, D. M. et al. Natural and anthropogenic changes in atmospheric CO_2 over the last 1000 years from air in Antarctic ice and firn. J. Geophys. Res. 101, 4115–4128 (1996).
47. Bender, M. et al. Climate correlations between Greenland and Antarctica during the past 100,000 years. Nature 372, 663–666 (1994).